Molecular and Electronic Structure of (L-Histidinato)pentammineruthenium(III) Chloride Monohydrate, $(NH_3)_5Ru^{III}(his)Cl_3 \cdot H_2O$. X-ray Structure, Single-Crystal Polarized Charge-Transfer Spectra, and ab Initio and Semiempirical Molecular Orbital Calculations

Karsten Krogh-Jespersen,* John D. Westbrook, Joseph A. Potenza,* and Harvey J. Schugar*

Contribution from the Department of Chemistry, Rutgers, The State University of New Jersey, New Brunswick, New Jersey 08903. *Received November 17, 1986*

Abstract: The synthesis, X-ray structure, and polarized single-crystal optical spectra are presented for the title complex. Crystals of $RuCl_3O_2N_8C_6H_{24} \cdot H_2O$ are orthorhombic, space group $P2_12_12_1$, with a = 7.113 (2) Å, b = 9.990 (1) Å, c = 25.717 (3) Å, V = 1827.2 (9) Å^3, Z = 4, and R_F (R_{wF}) = 0.061 (0.063) for 1339 reflections. The structure contains $(NH_3)_5Ru(his)^{3+}$ cations linked to lattice chloride ions and water molecules by an extensive network of hydrogen bonds. Five ammine and one histidine N atoms provide slightly distorted octahedral coordination for Ru. The Ru–N(his) bond length [2.020 (8) Å] is substantially shorter than the average Ru–N(ammine) distance [2.09 (2) Å] and the corresponding Ru–N(heterocycle) distances in several related pentammineruthenium(III) complexes. The histidine imidazole ring is staggered with respect to the four equatorial NH_3 ligands and is approximately perpendicular to a. Polarized single-crystal spectra of the title complex obtained at 80 K reveal that the low-energy LMCT absorption at 22 200 cm^{-1} (450 nm) is strongly polarized along the Ru–N(his) direction and suggest that the higher energy LMCT band at 33 000 cm^{-1} (303 nm) may exhibit similar polarization. Ab initio molecular orbital calculations were performed on $(NH_3)_5Ru^{III}$–imidazole with use of effective core potentials for the inner atomic electrons and valence basis sets of double-ζ quality. The ground state has been established as $^2d_{xz}$, where d_{xz} is the Ru(4d) orbital capable of interaction with the imidazole π-system; the unpaired electron is fully localized in this orbital. The σ-donation from imidazole (0.36e) is twice as large as that from any ammine (0.17e), but the imidazole π-donation is quite weak (0.06e). Geometry optimization yields good agreement between calculated and experimental Ru–N bond lengths. The relevant Ru parameters required for the semiempirical INDO/S method have been developed from atomic spectral data. Excited state calculations on $(NH_3)_5Ru^{III}$–5-methylimidazole provide assignments for the optical charge-transfer spectra as $\pi_1 \rightarrow d_{xz}$ and $\pi_2 \rightarrow d_{xz}$, where π_1 and π_2 are the two high-lying occupied imidazole π-orbitals. These two LMCT transitions are calculated at 21 200 cm^{-1} (472 nm) and 35 000 cm^{-1} (286 nm), respectively, and both have their largest transition moment components along the Ru–N(heterocycle) axis.

The modification of metalloproteins with one or more $(NH_3)_5Ru^{III}$ probes attached to histidine imidazole groups has facilitated elegant kinetic and thermodynamic studies of long-range electron transfer[1] in cytochrome c,[2,3] azurin,[4] and myoglobin.[5] The electronic structure and spectroscopic properties of this $(NH_3)_5Ru^{III}$–imidazole chromophore are pertinent to its use as an electron-transfer probe. For example, features of *optical* electron transfer (charge-transfer absorptions) may be directly related to the rate of *thermal* (ground state) electron transfer by the Marcus-Hush model.[6] Charge-transfer absorptions of $(NH_3)_5Ru^{III}$–imidazole(ate) complexes have been studied by several research groups.[7,8] The synthesis and characterization of these complexes have been developed by Taube and co-workers.[7] It was appreciated early on that the red shifts of both the weak visible [22 200 cm^{-1} (450 nm); $\epsilon \approx 200$] and the moderately intense near-UV absorption [33 000 cm^{-1} (303 nm); $\epsilon \approx 2000$] bands caused by imidazole methylation and/or deprotonation are diagnostic of ligand-to-metal charge-transfer (LMCT) absorptions.[8] Apparently similar absorptions are exhibited by $(NH_3)_5Ru^{III}$–purine complexes[9-12] in which the Ru(III) is bound to a N-donor of the imidazole-like portion of the purine.[13] Further details of this imidazole $\rightarrow$ Ru^{III} LMCT were revealed when energetic features of these absorptions were correlated with the qualitative[14] and calculated[15] effects of methylation and/or deprotonation on the upper occupied ligand π-orbitals of imidazole. Moreover, the observed intensity ratios of the visible and near-UV LMCT bands are in accord with the calculated coefficients at the imidazole N-donor site for the highest occupied (π_1, HOMO) and second highest occupied (π_2) molecular orbitals, leading to suggested assignments for the two bands as $\pi_1 \rightarrow$ Ru(d) and $\pi_2 \rightarrow$ Ru(d) LMCT, respectively.[15]

We report here the first detailed electronic structural and spectroscopic study of a Ru^{III}–imidazole complex including its crystallographic characterization, the experimental determination of the polarization for the lowest energy LMCT band, and theoretical results from ab initio and semiempirical molecular orbital calculations.

Experimental and Computational Section

1. Preparation of the Title Complex 1. The chiral complex was prepared by the method of Sundberg and Gupta using L-histidine instead

(1) Gray, H. B. *Science* **1986**, 948.
(2) Nocera, D. G.; Winkler, J. R.; Yocom, K. M.; Bordignon, E.; Gray, H. B. *J. Am. Chem. Soc.* **1984**, *106*, 5145.
(3) (a) Isied, S. S.; Kuehn, C.; Worosila, G. J. *J. Am. Chem. Soc.* **1984**, *106*, 1722. (b) Bechtold, R.; Kuehn, C.; Lepre, C.; Isied, S. S. *Nature (London)* **1986**, *322*, 286.
(4) (a) Margalit, R.; Kostic, N. M.; Che, C.-M.; Blair, D. F.; Chiang, H.-J.; Pecht, I.; Shelton, J. B.; Shelton, J. R.; Schroeder, W. A.; Gray, H. B. *Proc. Natl. Acad. Sci. U.S.A.* **1984**, *81*, 6554. (b) Kostic, N. M.; Margalit, R.; Che, C.-M.; Gray, H. B. *J. Am. Chem. Soc.* **1983**, *105*, 7765. (c) Gray, H. B. *Chem. Soc. Rev.* **1986**, *15*, 17.
(5) Crutchley, R. J.; Ellis, W. R., Jr.; Gray, H. B. *J. Am. Chem. Soc.* **1985**, *107*, 5002.
(6) Meyer, T. J. In *Progress in Inorganic Chemistry*; Lippard, S. J., Ed.; John Wiley & Sons, Inc.: New York, 1983; Vol. 30, p 389.
(7) Tweedle, M. F.; Taube, H. *Inorg. Chem.* **1982**, *21*, 3361.
(8) Sundberg, R. J.; Bryan, R. F.; Taylor, I. F., Jr.; Taube, H. *J. Am. Chem. Soc.* **1974**, *96*, 381.
(9) Clarke, M. J.; Taube, H. *J. Am. Chem. Soc.* **1974**, *96*, 5413.
(10) Clarke, M. J.; Taube, H. *J. Am. Chem. Soc.* **1975**, *97*, 1397.
(11) Clarke, M. J. *Inorg. Chem.* **1977**, *16*, 738.
(12) Clarke, M. J. *J. Am. Chem. Soc.* **1978**, *100*, 5068.
(13) Kastner, M. E.; Coffey, M. J.; Clarke, M. J.; Edmonds, S. E.; Eriks, K. *J. Am. Chem. Soc.* **1981**, *103*, 5747.
(14) Johnson, C. R.; Henderson, W. W.; Shepherd, R. E. *Inorg. Chem.* **1984**, *23*, 2754.
(15) Krogh-Jespersen, K.; Schugar, H. J. *Inorg. Chem.* **1984**, *23*, 4390.

0002-7863/87/1509-7025$01.50/0

Table I. Crystal and Refinement Data for **1**

formula	$RuCl_3O_3N_8C_6H_{26}$
fw	465.75
a, Å	7.113 (2)
b, Å	9.990 (1)
c, Å	25.717 (3)
V, Å^3	1827.2 (9)
space group	$P2_12_12_1$
Z	4
no. of ref used to detn cell constants	25 ($4.15 < \theta < 17.54$)
d_{calcd}, g/cm^3	1.693
d_{obsd}, g/cm^3	1.71 (1)
radiation used	graph. mono. Mo Kα (0.710 73 Å)
linear abs coeff, cm^{-1}	13.0
crystal dimns, mm	0.25 × 0.16 × 0.08
rel trans factor range	$0.93 < T < 1$
diffractometer	Enraf-Nonius CAD-4
data collection method	θ–2θ
2θ range, deg	$2 \le 2\theta \le 50$
temp, K	298 (1)
scan range, deg	$0.90 + 0.35 \tan \theta$
weighting scheme[a]	$w = 4(F_o)^2/[\sigma(F_o)^2]^2$
no. of std reflcns	3
% variation in std intens	±0.4
no. of unique data collected	1874
no. of data used in refinement	1339 [$F_o^2 \ge 2\sigma(F_o^2)$]
data: parameter ratio	7.0
final G.O.F.	1.57
final R_F, R_{wF}	0.061 (0.063)
systematic absences obsd	$h00$, $h = 2n + 1$; $0k0$, $k = 2n + 1$; $00l$, $l = 2n + 1$
data collected	hkl
final largest shift/esd	0.03
highest peak in final diff map, e/Å^3	1.11

[a] $[\sigma(F_o)^2]^2 = [S^2(C + R^2B) + (rF_o^2)^2]/(Lp)^2$, where S is the scan rate, C is the integrated peak count, R is the ratio of scan to background counting time, B is the total background count, and r is a factor used to downweight intense reflections. For this structure $r = 0.04$.

of D,L-histidine.[16] Slow vapor diffusion of ethanol into an aqueous solution of the complex yielded yellow–orange rectangular plates suitable for crystallographic and spectroscopic studies. Subsequent crystallographic analysis showed that the complex crystallized as the monohydrate, $(NH_3)_5(C_6H_9O_2N_3)RuCl_3 \cdot H_2O$. Presumably owing to loss of lattice water, the crystals turned opaque in air. A thin coating of mineral oil was sufficient to ensure crystal stability for the spectroscopic studies. Anal. Calcd for $C_6H_{26}O_3Cl_3N_8Ru$: C, 15.47; H, 5.64; N, 24.06; Cl, 22.83. Found: C, 15.44; H, 5.67; N, 23.37; Cl, 21.87.

2. Spectroscopic Measurements. Spectral measurements were made with a computer-interfaced spectrophotometer built by Aviv Associates that utilizes a Cary Model 14 monochromator and cell compartment. Polarization measurements were made with matched Glan-Thompson prisms that have a usable angular field of ≈ 15°. Separate polarizers in the sample and reference beams were rotated in unison by a chain drive mechanism. The light beam was directed normal to the (001) crystal face; the crystal was mounted in an evacuable dewar fitted with quartz windows. This face is the only one that is prominently developed. Minimum and maximum absorbances of the visible and near-UV bands were observed with the electric vector of the light beam directed along the crystallographic a and b axes, respectively. These are extinction directions for this orthorhombic crystal and thus are appropriate for polarization studies. The projection of the crystal spectra onto molecular electronic axes was accomplished by a locally modified version of a program obtained from Professor E. I. Solomon of Stanford University; further details are provided in the section devoted to spectroscopic results.

3. X-ray Diffraction Studies. A crystal of **1** was mounted along the a axis inside a glass capillary that contained a small amount of mother liquor well removed from the crystal. All diffraction measurements were made on an Enraf-Nonius CAD-4 diffractometer and with graphite-monochromated Mo Kα radiation. The Enraf-Nonius Structure Determination Package[17] was used for data collection, processing, and structure solution. Crystal data and additional details of the data collection and refinement are presented in Table I. Intensity data were collected and corrected for decay, absorption (empirical) and Lp effects.

The structure was solved by direct methods[18] and refined on F with full-matrix least-squares techniques. An E-map based on 409 phases from the starting set with the highest combined figure of merit revealed coordinates of the Ru and six ligand atoms. The remaining non-hydrogen atoms were located from successive difference Fourier maps. Following refinement of the heavy atoms, several H atoms were located on a difference map. Coordinates for the remaining H atoms were calculated assuming idealized bond geometries.[19] One water H atom could not be

Table II. Fractional Atomic Coordinates and Equivalent Isotropic Thermal Parameters for **1**

	x	y	z	B_{eq}, Å^2
Ru	0.2712 (2)	0.9570 (1)	0.83795 (4)	2.79 (2)
Cl(1)	0.7809 (7)	0.1341 (4)	0.7772 (2)	5.6 (1)
Cl(2)	0.2654 (8)	0.6950 (9)	1.0951 (2)	13.8 (2)
Cl(3)	0.323 (1)	1.3729 (5)	0.8229 (2)	11.3 (2)
O(1)	0.284 (2)	0.2751 (9)	1.0439 (4)	5.0 (3)
O(2)	0.314 (2)	0.1864 (2)	0.9648 (3)	4.2 (2)
O(3)	0.108 (3)	0.949 (2)	0.6779 (5)	14.4 (6)
N(1)	0.262 (2)	0.8286 (9)	0.8986 (3)	2.6 (2)
N(2)	0.046 (2)	0.859 (1)	0.8042 (5)	4.5 (3)
N(3)	0.468 (2)	0.837 (1)	0.8010 (5)	4.3 (3)
N(4)	0.282 (2)	1.084 (1)	0.7725 (4)	4.9 (3)
N(5)	0.494 (2)	1.064 (1)	0.8731 (5)	4.8 (3)
N(6)	0.078 (2)	1.080 (1)	0.8747 (5)	4.2 (3)
N(7)	0.263 (2)	0.745 (1)	0.9764 (4)	3.5 (3)
N(8)	0.513 (2)	0.411 (1)	0.9324 (5)	4.6 (3)
C(1)	0.283 (2)	0.853 (1)	0.9483 (5)	3.1 (3)
C(2)	0.239 (2)	0.689 (1)	0.8963 (5)	3.2 (3)
C(3)	0.234 (2)	0.635 (1)	0.9442 (5)	2.4 (3)
C(4)	0.207 (2)	0.496 (1)	0.9614 (6)	4.1 (3)
C(5)	0.385 (2)	0.422 (1)	0.9773 (5)	3.0 (3)
C(6)	0.327 (2)	0.279 (1)	0.9958 (5)	3.5 (3)

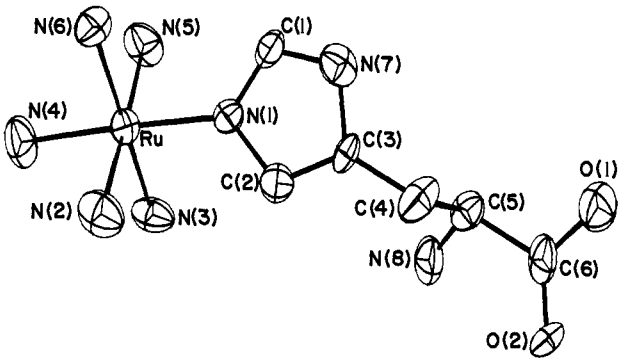

Figure 1. ORTEP view of the title complex **1** showing the atom-numbering scheme. Chloride anions and the lattice water molecule have been omitted for clarity.

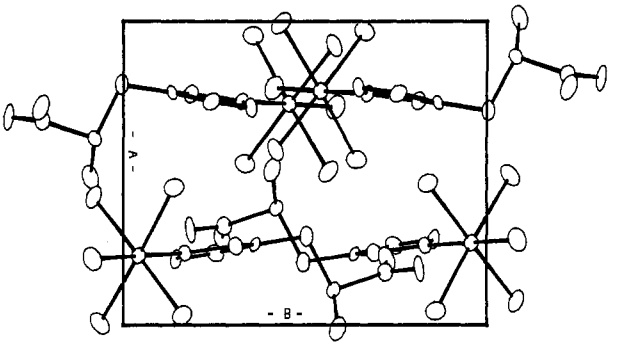

Figure 2. View along [001] of the $(NH_3)_5Ru(his)^{3+}$ cations in the unit cell. The imidazole groups are approximately perpendicular to the a axis (vertical direction); the b axis is horizontal.

(16) Sundberg, R. J.; Gupta, G. *Bioinorg. Chem.* **1973**, *3*, 39.
(17) Enraf-Nonius Structure Determination Package, Enraf-Nonius, Delft, Holland, 1983.
(18) Main, P.; Fiske, S. J.; Hull, S. E.; Lessinger, L.; Germain, G.; Declercq, J.-P.; Woolfson, M. M.; MULTAN 82. A System of Computer Programs for the Automatic Solution of Crystal Structures from X-ray Diffraction Data. University of York, England and Louvain, Belgium, 1982.
(19) Churchill, M. R. *Inorg. Chem.* **1973**, *12*, 1213.

Table III. Bond Distances (Å) and Angles (deg) in **1**

Ru–N(1)	2.020 (8)	Ru–N(6)	2.07 (1)	N(1)–C(2)	1.41 (1)	C(2)–C(3)	1.34 (1)
Ru–N(2)	2.07 (1)	O(1)–C(6)	1.28 (1)	N(7)–C(1)	1.31 (1)	C(3)–C(4)	1.47 (1)
Ru–N(3)	2.07 (1)	O(2)–C(6)	1.23 (1)	N(7)–C(3)	1.39 (1)	C(4)–C(5)	1.52 (2)
Ru–N(4)	2.111 (9)	N(1)–C(1)	1.31 (1)	N(8)–C(5)	1.47 (2)	C(5)–C(6)	1.57 (2)
Ru–N(5)	2.12 (1)						

N(1)–Ru–N(2)	90.0 (5)	N(3)–Ru–N(6)	178.9 (5)	N(7)–C(3)–C(4)	125.8 (9)
N(1)–Ru–N(3)	90.5 (5)	N(4)–Ru–N(5)	90.5 (5)	C(2)–C(3)–C(4)	131 (2)
N(1)–Ru–N(4)	177.7 (4)	N(4)–Ru–N(6)	91.7 (5)	C(3)–C(4)–C(5)	116 (1)
N(1)–Ru–N(5)	90.9 (5)	N(5)–Ru–N(6)	90.1 (4)	N(8)–C(5)–C(4)	110 (1)
N(1)–Ru–N(6)	90.3 (4)	C(1)–N(1)–C(2)	104.1 (8)	N(8)–C(5)–C(6)	109 (2)
N(2)–Ru–N(3)	93.2 (4)	Ru–N(1)–C(1)	129.0 (7)	C(4)–C(5)–C(6)	108 (1)
N(2)–Ru–N(4)	88.6 (5)	Ru–N(1)–C(2)	126.9 (7)	O(1)–C(6)–O(2)	127 (1)
N(2)–Ru–N(5)	177.6 (5)	C(1)–N(7)–C(3)	109.8 (9)	O(1)–C(6)–C(5)	113 (1)
N(2)–Ru–N(6)	87.7 (6)	N(1)–C(1)–N(7)	112 (1)	O(2)–C(6)–C(5)	121 (2)
N(3)–Ru–N(4)	87.8 (5)	N(1)–C(2)–C(3)	110.9 (9)		
N(3)–Ru–N(5)	89.1 (5)	N(7)–C(3)–C(2)	103.4 (8)		

located with certainty and was not included in the refinement. H-atom temperature factors were set equal to $1.3B_N$ where N is the atom bonded to H; H-atom parameters were not refined. At the final stages of refinement, both enantiomers were refined anisotropically; the enantiomer with L-histidine converged with a significantly lower value of R_{wF}, indicating that this choice is correct. Final values of R_F and R_{wF} were 0.061 and 0.063, respectively. Atomic parameters are listed in Table II while views of the structure and packing projected on the (001) face are given in Figures 1 and 2, respectively.

The data in Table II show very large thermal parameters for two of the chloride ions and for the lattice water molecule, suggesting that these species may be disordered. The largest and third largest peaks in the final difference Fourier map are located 0.59 and 0.69 Å from Cl(2) and support this view. Attempts to treat a chloride disorder by assuming that Cl(2) and Cl(3) each occupied two sites yielded oscillating parameters, higher coordinate esd's, and no significant improvement between observed and calculated structure factors. Finally, because of the possibility that loss of solvent led to an apparent disorder, a second data set was collected with use of freshly prepared, slowly grown crystals; the structure obtained was equivalent, within experimental error, to that reported here. We conclude that Cl(2), Cl(3), and the water molecule are loosely held in the lattice and that this results in larger than expected esd's of coordinates and derived parameters for a structure at this level of refinement. Lists of anisotropic thermal parameters, H atom coordinates, and observed and calculated structure factors are available.[20]

4. Computational Details. Ab initio molecular orbital (MO) calculations have been performed on $(NH_3)_5Ru^{III}$–imidazole, NH_3, and imidazole with use of an extended version of the HONDO/GAMESS program packages[21] provided to us by Dr. M. Krauss of the National Bureau of Standards. Wave functions for closed shell singlet states were calculated with use of the standard single determinant restricted Hartree–Fock method prescribed by Roothaan,[22a] whereas the unrestricted procedure due to Pople and Nesbet was used for the doublet states.[22b] Electronic population indices were obtained with use of conventional Mulliken partitioning techniques.[22c]

The inner core electrons of Ru ($1s^2 2s^2 2p^6 3s^2 3p^6$), C ($1s^2$), and N ($1s^2$) were replaced by the ab initio effective core potentials generated by Hay and Wadt (Ru)[23a] or Stevens, Basch, and Krauss (C, N).[23b] The valence electrons were described with the basis sets developed specifically for use with these potentials.[23a,b] The contraction for Ru was of double-ζ quality (3s, 3p, 4d) → [1, 1, 1/2, 1/3, 1] with the most diffuse Gaussian function serving as the outer basis function in the p and d sets; all six Cartesian d-components were retained in the basis. For H, the standard STO-3G basis set of Hehre, Stewart, and Pople was used.[23c] The basis sets for C and N share s and p Gaussian exponents but utilize different expansion coefficients. Both the minimal basis contraction of four Gaussians as well as the split valence description (4s, 4p) → [3, 1/3, 1] were used as described below.

The geometry of the entire $(NH_3)_5Ru^{III}$–imidazole complex was fully optimized with the effective potentials, the double-ζ Ru basis, and the minimal basis sets on C, N, and H described above, subject only to a C_s point group symmetry constraint. Justification for this symmetry restriction may be derived from the present crystallographic study (vide infra). Thus, these calculations on the Ru chromophore involved 80 basis functions and 71 electrons. A single-point calculation on the optimized geometry utilized, in addition, the split valence basis for the C and N atoms and thus contained 120 basis functions. Finally, the geometries of the ammonia (C_{3v}) and imidazole (C_s) free ligands were also optimized with both the minimal and split-valence descriptions.

Semiempirical calculations on the electronically excited states of $(NH_3)_5Ru$–5-methylimidazole^{3+}, $Ru(NH_3)_6^{3+}$, and 5-methylimidazole have also been carried out with a locally modified version of an INDO program provided by Professor M. Zerner, University of Florida, Gainesville.[24] We are in the process of developing parameters suitable for the calculation of spectroscopic properties in metallo-organic complexes containing inter alia Ru. We shall present a more detailed description of the methodology and optimal parameters after extensive testing and performance evaluation have taken place.[25] The parameters used in this study should, therefore, be considered preliminary, but they are not expected to be significantly different from the final set.

The one-center electron–electron repulsion integrals for Ru(0) were evaluated from atomic data[26a] by using the methods of Anno and Teruya, and Hinze and Jaffe.[26b] The values (in eV) are the following: $\gamma_{sp} = 4.58$; $\gamma_{sd} = 5.13$; $\gamma_{dd} = 7.68$; $G^1(sp) = 2.48$; $G^2(sd) = 0.99$; $G^1(pd) = 0.36$; $G^3(pd) = 0.49$; $F^2(pp) = 1.12$; $F^2(pd) = 1.47$; $F^2(dd) = 6.36$; and $F^4(dd) = 4.97$. The ionization potentials were also derived from atomic data[26a] as EI(s) = 7.38 eV ($Kr4d^75s^1 \rightarrow Kr4d^7$), EI(p) = 4.21 eV ($Kr4d^75p^1 \rightarrow Kr4d^7$), and EI(d) = 8.97 eV ($Kr4d^75s^1 \rightarrow Kr4d^65s^1$). The basis set for Ru consisted of single-ζ Slater orbitals with exponents of 2.95 (4d) and 1.40 (5s and 5p). The one-center electron repulsion integrals and ionization potentials for H, C, and N were those of ref 24a, except that the EI(p) for N was lowered to 13.0 eV. Standard Slater exponents were used for H, C, and N orbitals.

The INDO/1S scheme[24a] was used with two-center electron-repulsion integrals evaluated by the Mataga-Nishimoto formula as modified by Weiss.[27] The screening factors applied in the evaluation of overlap integrals were $k_\sigma = 1.00$ and $k_\pi = 0.64$ in the complex but $k_\pi = 0.585$ in the free ligand.[24a] The "resonance" integral parameters for Ru were $\beta(4d) = -32.0$ eV, $\beta(5s) = \beta(5p) = -4.0$ eV; standard values were used for C and H[24] but $\beta(s) = \beta(p)$ for N was increased from −26.0 eV[24] to −24.0 eV.

The fixed geometries used for the semiempirical calculations on $(NH_3)_5Ru$–5-methylimidazole^{3+} and 5-methylimidazole were based on coordinates from the present X-ray determination, suitably reoriented and averaged to exhibit C_s symmetry. The C–H bond lengths were 1.08 Å in the imidazole portion and 1.09 Å in the methyl group; in addition, the C–C(methyl) and N–H bond lengths were increased to 1.52 and 1.01 Å, respectively.[28] The geometry of $Ru(NH_3)_6^{3+}$ was based on the reported

(20) Supplementary material.
(21) Dupuis, M.; King, H. F. *Int. J. Quant. Chem.* **1977**, *11*, 613; *J. Chem. Phys.* **1978**, *68*, 3998.
(22) (a) Roothaan, C. C. J. *Rev. Mod. Phys.* **1951**, *23*, 69. (b) Pople, J. A.; Nesbet, R. K. *J. Chem. Phys.* **1954**, *22*, 571. (c) Mulliken, R. S. *J. Chem. Phys.* **1955**, *23*, 1833. (d) Roothaan, C. C. J. *Rev. Mod. Phys.* **1960**, *32*, 179.
(23) (a) Hay, P. J.; Wadt, W. R. *J. Chem. Phys.* **1985**, *82*, 270. (b) Stevens, W. J.; Basch, H.; Krauss, M. *J. Chem. Phys.* **1984**, *81*, 6026. (c) Hehre, W. J.; Stewart, R. F.; Pople, J. A. *J. Chem. Phys.* **1969**, *51*, 2657.
(24) (a) Zerner, M. C.; Loew, G. H.; Kirchner, R. F.; Mueller-Westerhoff, U. T. *J. Am. Chem. Soc.* **1980**, *102*, 589. (b) Zerner, M.; Bacon, A. D. *Theor. Chim. Acta* **1979**, *53*, 21. (c) Ridley, J.; Zerner, M. *Theor. Chim. Acta* **1973**, *32*, 11; **1976**, *42*, 233; Zerner, M., private communication.
(25) Westbrook, J. D.; Krogh-Jespersen, K., to be submitted for publication.
(26) (a) Moore, C. E. *Natl. Bur. Std. Circ. (U.S.)* **1958**, *467*, 3. (b) Anno, T.; Teruya, H. *Theor. Chim. Acta* **1971**, *21*, 127; *J. Chem. Phys.* **1970**, *52*, 2840. Anno, T.; Sakai, Y. *J. Chem. Phys.* **1972**, *57*, 4910. Hinze, J.; Jaffe, H. H. *J. Chem. Phys.* **1963**, *38*, 1834.
(27) Mataga, M.; Nishimoto, K. *Z. Phys. Chem.* **1957**, *13*, 140. Weiss, K., unpublished results.

structure.[29] The ground-state wave functions were generated by using the restricted closed[22a] or open[22d] shell methods of Roothaan. The excited states were then obtained from extensive configuration interaction calculations by using configurations singly excited relative to the ground state; about 120 configurations were included in each symmetry block. Only configurations preserving the spin orientation of the excited electron were included in the doublet calculations. It was ascertained that reasonable convergence of the configuration interaction expansion had been obtained with this number of configurations. Finally, oscillator strengths were calculated in the dipole length approximation including the one-center sp and pd atomic terms.

Results and Discussion

Description of the Structure. The structure consists of discrete, approximately octahedral $(NH_3)_5Ru^{III}$his cations separated by lattice chloride ions and water molecules. Selected bond distances and angles are listed in Table III. Except as noted below, structural parameters of the $Ru^{III}N_6$ unit are comparable to those reported for the related complexes $(NH_3)_5Ru(pyrazine)^{3+}$ (**2**),[30a] $(NH_3)_5$(*N*-methylpyrazinium)Ru^{III} (**3**),[30b] $(NH_3)_5RuL^{3+}$ (L = 7-hypoxanthine (**4**),[13] 9-(7-methylhypoxanthine) (**5**)[13]), and *cis*-$(NH_3)_4Ru(isonicotinamide)_2^{3+}$ (**6**).[31a] As has been observed for **2–6**, the Ru–N(heterocycle) bond distance is somewhat shorter than the average Ru–NH_3 distance. Thus, the added effect of metal d(π)–ligand p(π) bonding may be detected for imidazole ligation as well. This effect is generally small for Ru(III) complexes and, except for **1**, is not much larger than the realistic uncertainties for comparing differences in bond distances. The Ru–N(his) bond length in **1** [2.020 (8) Å] is, however, substantially shorter than the corresponding Ru–N(heterocycle) distances in **2–6** [2.076 (8), 2.08 (1), 2.087 (9), 2.094 (6), and 2.093 (4) Å, respectively]. We attribute the relatively short Ru–N(his) bond length to the *electron-donating* role of the imidazole ligand which is substantiated by the computational studies (vide infra). The other N(heterocyclic) ligands are believed to be less potent σ-donors than histidine imidazole. Moreover, the histidine imidazole is a π-*donor* whereas the other N(heterocyclic) ligands are either weaker π-donors or formal π-acceptors.

The histidine imidazole ring is essentially planar and oriented such that it bisects approximately the N(2)–Ru–N(3) and N(5)–Ru–N(6) bond angles; this result, which shows that the imidazole plane is staggered with respect to the four equatorial NH_3 ligands, is clearly seen in the packing diagram (Figure 2). The planes of the aromatic ligands in **2–6** also either closely or precisely (crystallographically required) bisect pairs of N–Ru–N bond angles in the plane normal to the Ru–N(heterocycle) bond. This preference for the staggered conformation seems to be general and presumably arises from steric and/or electronic factors. In **1**, examination of Dreiding models reveals steric interference between ammine and heterocycle H atoms only in the eclipsed conformation.

A structural study of a $[Cl_5Ru(imidazole)]^{2-}$ complex was published[31b] after our manuscript was submitted for publication. In agreement with the results reported above, the imidazole unit in this latter complex also has the staggered conformation, the Ru^{III}–N(imidazole) bond length is relatively short [2.044 (12) Å], and the trans Ru–Cl bond [2.446 (4) Å] is elongated relative to the remaining Ru–Cl bonds [2.364 (3), 2.378 (3) Å].

The L-histidine residue adopts the extended conformation about C(4)–C(5) with the imidazole group trans to the carboxylate and gauche to the ammine group. This conformation is similar to that reported[32] for the orthorhombic form of L-histidine except that, for the free amino acid, the imidazole ring is oriented so as to form a weak intramolecular hydrogen bond between a ring N atom and the NH_3 group of the amino acid. The various species in the lattice are joined by an extensive network of hydrogen bonds involving all three chloride ions, the water molecule, the carboxylate O atoms, and several NH_3 groups of the cations. Details of the hydrogen bonding network are given in Table IV.

Table IV. Possible Hydrogen-Bonding Contacts in **1**

donor (D)[a]	hydrogen (H)	acceptor (A)	D–H···A, deg	D···A, Å	H···A, Å	D–H, Å
O(3)^{i}	HO(31)	Cl(3)	136	3.16 (2)	2.42	0.94
N(4)	HN(42)	Cl(3)	163	3.18 (1)	2.21	0.99
N(5)^{ii}	HN(52)	Cl(1)	148	3.27 (1)	2.43	0.94
N(5)^{ii}	HN(53)	O(2)	163	2.95 (2)	2.00	0.97
N(6)^{iii}	HN(62)	Cl(1)	159	3.32 (1)	2.41	0.96
N(7)	HN(71)	Cl(2)	161	3.093 (9)	2.16	0.97
N(8)^{iv}	HN(81)	O(1)	157	2.74 (1)	1.83	0.97
N(8)^{v}	HN(83)	Cl(3)	144	3.14 (1)	2.31	0.96

[a] Symmetry transformations: i = $-x$, $^1/_2 + y$, $^3/_2 - z$; ii = x, $y - 1$, z; iii = $x + 1$, $y - 1$, z; iv = $x - ^1/_2$, $^1/_2 - y$, $2 - z$; v = x, $1 + y$, z.

Table V. Experimental and Calculated Bond Lengths (Å)

	complex	free ligand		
	X-ray (**1**)	minimal basis	minimal basis	split valence	MW[a]
N(1)–C(1)	1.31 (1)	1.42	1.415	1.317	1.314
C(1)–N(7)	1.31 (1)	1.43	1.472	1.379	1.364
N(7)–C(3)	1.39 (1)	1.48	1.468	1.395	1.377
C(2)–C(3)	1.34 (1)	1.48	1.479	1.384	1.364
C(2)–N(1)	1.41 (1)	1.48	1.482	1.397	1.382
Ru–N(1)	2.020 (8)	1.99			
Ru–N(2)	2.07 (1)	2.15			
Ru–N(3)	2.07 (1)	2.15			
Ru–N(4)	2.111 (9)	2.18			
Ru–N(5)	2.12 (1)	2.15			
Ru–N(6)	2.07 (1)	2.15			

[a] MW refers to the gas-phase microwave structure, ref 33.

Our $(NH_3)_5Ru^{III}$–imidazole model complex used in the ab initio MO calculations possesses C_s symmetry; i.e., the plane of the imidazole ring bisects the N(2)–Ru–N(3) and N(5)–Ru–N(6) angles. The coordinate system has the imidazole–Ru–N(4) plane forming the xy plane with the x axis essentially along Ru–N(1), the y axis bisecting the N(2)–Ru–N(3) and N(5)–Ru–N(6) angles, and the z axis perpendicular to the imidazole plane bisecting the N(2)–Ru–N(6) and N(3)–Ru–N(5) angles. Calculations with different combinations of basis sets have been performed at various fixed geometries. For the discussion of the ground-state electronic structure, we have chosen to use results from the wave function generated by the large basis set at the optimized geometry provided by the smaller basis set (see Computational Details). There are noticeable differences in the electronic populations given by the various basis sets, but they are mostly minor and do not affect the general description of the bonding in the complex. In particular, the ground state of the complex is in all cases found to be $^2A''$ with the unpaired electron residing in the Ru($4d_{xz}$) orbital.

The optimized geometry shows a Ru(III) environment with only small distortions from octahedral symmetry except for the Ru–N(1) bond which is calculated to be quite short at 1.99 Å. The Ru–N(4) bond trans to this is calculated to be 2.18 Å, slightly longer than the values obtained for the remaining Ru–N bonds [Ru–N(2) = Ru–N(3) = Ru–N(5) = Ru–N(6) = 2.15 Å]. These calculated distances compare favorably in terms of magnitudes and trends with those determined crystallographically (Table III) and with the Ru–N bond length of 2.104 (4) Å in $Ru(NH_3)_6^{3+}$,[29] although the calculated asymmetry between the Ru–N(4) and Ru–N(1) bond lengths appears exaggerated. All calculated N–Ru–N angles are within 2° of the ideal values for an octahedron, also in accordance with the present crystal structure.

The imidazole geometry is not well described with the pseudopotentials and the minimal basis set, however. The skeletal bond lengths are uniformly too long by about 0.1 Å at this level of calculation (Table V) The split valence basis set and pseudopotentials provide a geometry in far better agreement with the

(28) Pople, J. A.; Gordon, M. *J. Am. Chem. Soc.* **1967**, *89*, 4253.
(29) Stynes, H. C.; Ibers, J. A. *Inorg. Chem.* **1971**, *10*, 2304.
(30) (a) Gress, M. E.; Creutz, C.; Quicksall, C. O. *Inorg. Chem.* **1981**, *20*, 1522. (b) Wishart, J. F.; Bino, A.; Taube, H. *Inorg. Chem.* **1986**, *25*, 3318.
(31) (a) Richardson, D. E.; Walker, D. D.; Sutton, J. E.; Hodgson, K. O.; Taube, H. *Inorg. Chem.* **1979**, *18*, 2216. (b) Keppler, B. K.; Wehe, D.; Endres, H.; Rupp, W. *Inorg. Chem.* **1987**, *26*, 844.
(32) Madden, J. J.; McGandy, E. L.; Seeman, N. C. *Acta Crystallogr.* **1972**, *B28*, 2377.

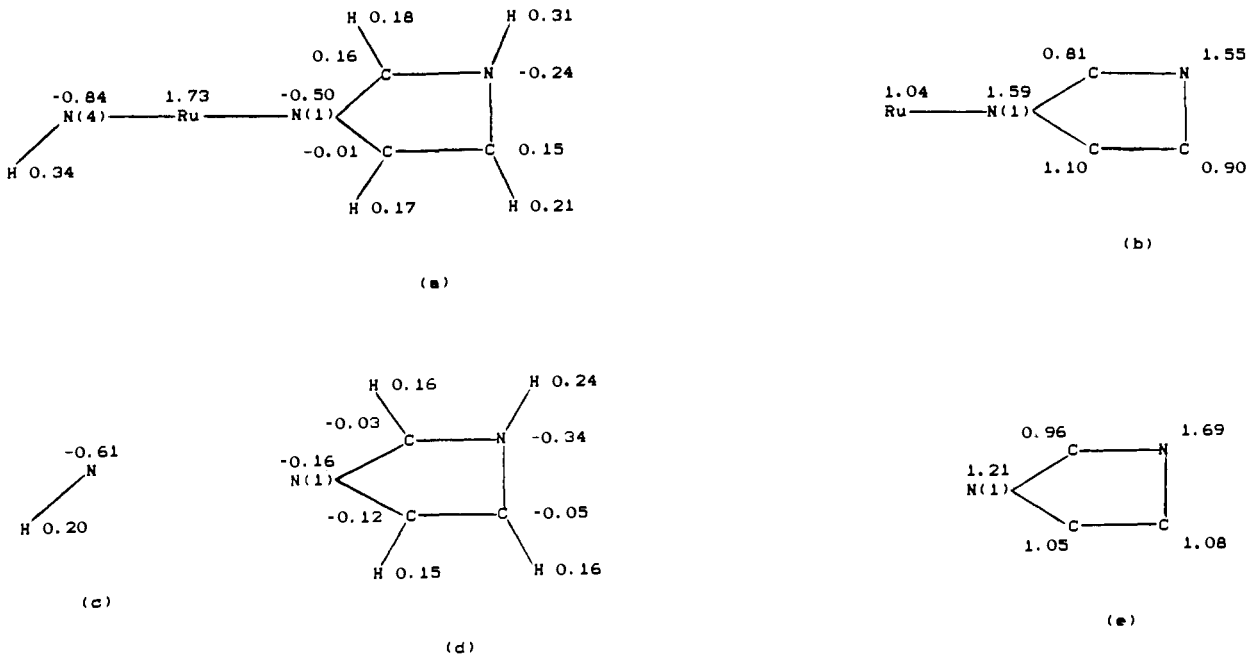

Figure 3. Calculated (a) net charges in $(NH_3)_5Ru^{III}$–imidazole, (b) π-population in $(NH_3)_5Ru^{III}$–imidazole, (c) net charge in NH_3, (d) net charge in imidazole, and (e) π-population in imidazole. Values were calculated with the Mulliken partitioning technique and the double-ζ basis set on the optimized geometries as described in the text.

present experimental data and, in particular, the imidazole structure determined by gas-phase microwave spectroscopy.[33] Changes in geometry should, however, be reproduced reliably by even the minimal basis set. Inspection of Table V shows that the changes in imidazole geometry upon complexation to Ru(III) are in fact small (<0.04 Å). So are the structural changes in the ammine ligands where all the N–H bonds lengthen by just 0.01 Å from the free ligand (1.045 Å) to the complex (1.055 Å).

Some results from the Mulliken population analysis are displayed in Figure 3. The calculated electronic distribution leads to an actual positive charge of 1.73 on the formally triply charged Ru ion; i.e., 1.27 electrons have been donated formally to the Ru atom. Comparisons with the charge distribution calculated for the free ligands show that on the average each NH_3 group has donated 0.17e while the imidazole has donated 0.42e to the Ru atom. The atomic charge distributions in the imidazole and ammine ligands become polarized toward the ligating N atoms, which actually are indicated to acquire additional negative charge in the complex (0.33e in imidazole, 0.23e in NH_3) relative to the free ligands. The Mulliken population analysis shows the H atoms in NH_3 and the C atoms in imidazole to be the donors of this transferred negative charge. Further analysis of the calculated electron populations indicates that the total of 0.42e transferred from the imidazole to the Ru consists of 0.36e σ-donation and only 0.06e π-donation. On the Ru atom, most of the charge is accepted into the formally unoccupied d_{x^2} (0.45e) and d_{yz} (0.50e) orbitals; in addition, a net of 0.11e resides in the 5s orbital, whereas very little charge accumulates in the 5p orbitals (0.07e). The population in the $4d_{xz}$ orbital, the formally half-filled d-orbital which overlaps with the imidazole π-system, is only 1.04e in accordance with the small imidazole π-donation noted above.

There are three high-lying occupied orbitals in imidazole of importance in Ru–imidazole bonding; two are of π-symmetry (π_1, π_2) and one is of σ-symmetry (n), the lone pair on N(1). The HOMO, π_1, would be the natural orbital to interact with the half-filled d_{xz} orbital, but π_1 has a very small coefficient on N(1), the primary site of Ru–imidazole interaction.[15] The second highest occupied MO, π_2, is the π-orbital with very large coefficients on N(1) and N(7)[15] and the composition of π_1 and π_2 in the complex shows that π_2 mixes far more with d_{xz} than π_1 does. This interaction is also reflected in the orbital energies for π_1 and π_2 in the complex compared with the free ligand. In free imidazole, we calculate the orbital energies of π_1 and π_2 at −8.62 eV and −10.52 eV, respectively. Assuming Koopmans' theorem is valid,[34a] these values translate into ionization potentials of 8.62 and 10.52 eV, in excellent agreement with the values of 8.71 and 10.3 eV derived from the photoelectron spectrum.[34b] The π_1–π_2 free ligand separation of 1.90 eV increases to 2.90 eV in the complex. The π_2–n separation increases even more from 1.16 eV in the free ligand to 2.56 eV in the complex. Thus, a rather strong Ru–N(1) $d(\sigma)$–$n(sp^2)$ type interaction is indicated by the σ-charge transferred, the preferential stabilization of the N(1) lone pair, and the short Ru–N(1) internuclear separation (calculated and observed). The $d(\pi)$–$p(\pi)$ interaction is modest, to some extent because of the absence of a good imidazole donor orbital: π_2 is too stable in the ligand and it is not fully localized on N(1). The Ru–ammine bonds are longer since they involve sp^3-type lone pairs and no π-type interaction. It appears that the imidazole ligand displays the orientation in the crystal that is sterically as well as electronically most favorable.

Spectroscopic Results. From Figure 2, which shows the packing of **1** projected on the (001) face, it is apparent that the crystallographic *a* axis is oriented approximately normal both to the Ru–N(1) bond direction and the imidazole plane. Examination of this crystal face with a polarizing microscope revealed a marked orange/faint yellow dichroism with the electric vector of the incident light parallel respectively to *b* and *a*. The (010) face also exhibited orange/pale yellow dichroism when the electric vector was oriented parallel to *c* and *a*, respectively. For an orthorhombic crystal, the lattice symmetry fixes the optical extinctions along the *a*, *b*, and *c* directions and requires that the four molecules of the unit cell are spectroscopically (and magnetically) equivalent along these directions.[35] Polarized electronic spectra must be measured along these crystallographic axes and then related to the spectra that would be obtained if the polarized light could be directed along appropriate molecular electronic axes. This process is straightforward here due to an unusually favorable packing of this geometrically regular complex.

(33) Christen, D.; Griffiths, J. H.; Sheridan, J. *Z. Naturforsch.* **1982**, *37a*, 1378.

(34) (a) Koopmans, T. C. *Physica (Utrecht)* **1934**, *1*, 104. (b) Craddock, S.; Findlay, R. H.; Palmer, M. H. *Tetrahedron* **1973**, *29*, 2173. Ramsey, B. G. *J. Org. Chem.* **1979**, *44*, 2093.

(35) Bencini, A.; Gatteschi, D. In *Transition Metal Chemistry*; Melson, G. A., Figgis, B. N., Eds.; Marcel Dekker Inc.: New York, 1982; Vol. 8, p 11.

Table VI. Crystallographic Coordinates for the Polarized Light Electric Vector (a, b, c) and Molecular X, Y, Z

vector	$(x, y, z)^a$	vector	$(x, y, z)^a$
a	(14.06, 0, 0)	X	(0.443, 6.351, −3.003)
b	(0, 10.01, 0)	Y	(10.9, 4.742, 1.636)
c	(0, 0, 3.89)	Z	(8.896, −6.114, −1.851)

Squares of the Projections of Molecular XYZ Along Crystallographic abc

$a = 0.001X + 0.598Y + 0.400Z$

$b = 0.403X + 0.224Y + 0.373Z$

$c = 0.597X + 0.177Y + 0.226Z$

[a] Multiplied by 100.

We define an orthogonal coordinate system[36] with molecular X parallel to the Ru–N(1) vector, molecular Y perpendicular to X and essentially along the Ru–N(2) vector, and molecular Z perpendicular to both X and Y and in the general direction of the Ru–N(3) vector. Owing to the nearly octahedral coordination geometry about Ru, Y and Z of the orthogonal coordinate system lie close to the Ru–N(2) and Ru–N(3) vectors. The intensity of an electric dipole absorption depends upon the square of the transition moment integral and therefore on the projections along the crystal abc axes of the squares of the M_x, M_y, M_z components of the electric dipole moment operator. The crystallographic coordinates of the XYZ and abc axes, and the squares of the calculated projections of the molecular XYZ axes along the crystal abc axes are listed in Table VI. Table VI merely quantifies the visually observable result from Figure 2 that the Ru–N(1) bond (molecular X) has approximately zero projection along the a axis and is mainly projected along b and c (40% and 60%, respectively).

The solution spectra of $(NH_3)_5Ru$(D,L-histidine)$^{3+}$ include absorptions at 22 200 cm^{-1} (450 nm, ϵ = 290) and 33 000 cm^{-1} (303 nm, ϵ = 2100).[16] These bands have been assigned as LMCT by Taube and co-workers[7,8] and more specifically by other workers as LMCT originating from the imidazole π_1 and π_2 orbitals, respectively.[14,15] The absorption at 33000 cm^{-1} has a high-energy shoulder whose intensity is difficult to estimate accurately. This shoulder must in part correspond to an absorption of the "parent" $(NH_3)_6Ru^{3+}$ complex at ≈36 400 cm^{-1} ($\epsilon \approx 500$), which may be a weak CT band.[37] A large number of doublet and quartet excited states arising from the $(t_{2g})^5$ configuration are associated with the relatively weak overlapping absorptions exhibited by the "parent" complex in the 20000–40000-cm^{-1} region.[37] These absorptions are easily obscured by LMCT for most Ru(III) complexes in general and for the $(NH_3)_5Ru$(imidazole)$^{3+}$ complexes in particular.

Before we discuss the results of the spectral calculations for $(NH_3)_5Ru$(5-methylimidazole)$^{3+}$, our model for the title complex, it is advantageous to consider briefly the electronic spectral properties of $Ru(NH_3)_6^{3+}$ and 5-methylimidazole. The octahedral $Ru(NH_3)_6^{3+}$ species is calculated to be optically silent below ≈31 000 cm^{-1}.[37,38] The excited d–d states are calculated at 31 750 cm^{-1} (doubly degenerate), 36 800 cm^{-1} (doubly degenerate), 38 000 cm^{-1}, and 44 700 cm^{-1} but all these transitions are calculated to have oscillator strengths of $f < 10^{-4}$; N → Ru LMCT transitions with noticeable intensity ($f \approx 0.01$) appear at 51 800 cm^{-1} and above. The experimental spectra[37] show steadily increasing absorption from about 25 000 cm^{-1} with a shoulder near 31 000 cm^{-1} and increasing featureless absorption above 41 000 cm^{-1}. In 5-methylimidazole, the lowest calculated singlet absorption is of n → π^* character at 36 800 cm^{-1} (f = 0.016), followed by the first

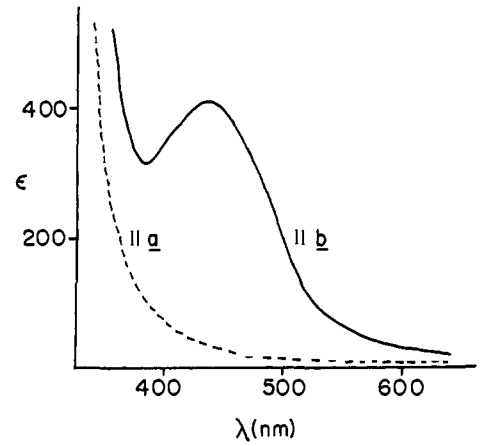

Figure 4. Polarized single-crystal spectra of **1** at 80 K with the electric vector oriented along b (solid line) or a (dotted line).

$\pi \rightarrow \pi^*$ transition at 43 300 cm^{-1} (f = 0.140). Experimental absorption spectra of imidazole and alkylated imidazoles[39] show no signs of the n → π^* transition as an identifiable peak but do display rising $\pi \rightarrow \pi^*$ absorption from 40 000 cm^{-1} with a peak above 45 000 cm^{-1} ($\epsilon \approx$ 15 000). Thus, the calculated transitions for $Ru(NH_3)_6^{3+}$ and 5-methylimidazole are in good agreement with observed spectra and, in particular, any low-energy transitions (below 30 000 cm^{-1}) in the title complex must clearly be the result of ligand–metal interactions.

The lowest optical absorption for the $(NH_3)_5Ru$(5-methylimidazole)$^{3+}$ complex is calculated at 21 200 cm^{-1} (f = 0.025), far below absorptions of the individual chromophores.[40] Examination of the configuration interaction eigenvectors reveals that this absorption is a very pure (98%) $\pi_1 \rightarrow Ru(4d_{xz})$ LMCT transition. An analogous second, also very pure (94%) but more intense LMCT transition is calculated at 35 000 cm^{-1} (f = 0.128) and is assigned as $\pi_2 \rightarrow d_{xz}$; its far larger intensity agrees qualitatively with the larger electron density present on N(1) in π_2 compared with π_1.[15] The solution spectra of $(NH_3)_5Ru$(5-methylimidazole)$^{3+}$ are nearly identical with those of the title complex (vide supra) and include absorptions at 21 000 cm^{-1} (ϵ = 267) and 33 000 cm^{-1} (ϵ = 2020).[7] Not only the calculated absolute frequencies but also the relative intensities of the two charge-transfer bands (f_{calcd} = 0.128/0.025 = 5.1; f_{obsd} = 2020/267 = 7.6) match experimental values well. For the $\pi_1 \rightarrow d_{xz}$ LMCT, the transition moment along the x-direction, the Ru–N(1) axis, is twice as large as that along the y-direction (1.45 D vs. 0.69 D), whereas for the $\pi_2 \rightarrow d_{xz}$ transition, this ratio is closer to six (2.75 D vs. 0.47 D along x and y, respectively). The localized imidazole $\pi \rightarrow \pi^*$ transition is calculated near 41 600 cm^{-1} (f = 0.155) and metal localized transitions are scattered throughout the region above 32 000 cm^{-1} with slightly larger calculated intensities (f = 10^{-3}–10^{-4}) than in the hexammine complex. This is a consequence of configurational mixing and intensity borrowing from the intense $\pi_2 \rightarrow d_{xz}$ and $\pi \rightarrow \pi^*$ transitions, and one or more of these d–d type transitions may be responsible for the shoulder observed to the high-energy side of the 33 000-cm^{-1} band.

The observed polarized single-crystal electronic spectra of **1** at 80 K (Figure 4) reveal that the 22 200 cm^{-1} (450 nm) absorption is strongly polarized along the Ru–N(1) bond direction. The higher energy LMCT absorption at 33 000 cm^{-1} (303 nm) also may exhibit similar polarization, but the presence of overlapping and perhaps oppositely polarized absorptions (vide supra) are a complicating feature. The observed and calculated polarization of the 22 200-cm^{-1} band primarily along the Ru–N(1) direction makes particular sense if the Ru(III) d-vacancy specifically is the one (d_{xz}) that participates in the Ru(III) d(π)–imidazole p(π) back-bonding, as the calculations strongly suggest. The exact

(36) This coordinate system (X, Y, Z) is related to the coordinate system (x, y, z) used in electronic structure calculations as follows: X and x are identical, Y and Z are rotated 45° around the $X(x)$ axis relative to y and z, and the labels are, in addition, interchanged.

(37) Navon, G.; Sutin, N. *Inorg. Chem.* **1974**, *13*, 2159.

(38) There are two low-lying states calculated near 250 cm^{-1} above the ground state. These states correspond to alternative occupancies of the five d-electrons within the quasidegenerate t_{2g} set. For other theoretical work on the optical spectra of $Ru(NH_3)_6^{3+}$ see: Daul, C.; Goursot, A. *Inorg. Chem.* **1985**, *24*, 3554. Ondrechen, M. J.; Ratner, M. A.; Ellis, D. E. *J. Am. Chem. Soc.* **1981**, *103*, 1656. Guenzburger, D.; Garnier, A.; Danon, J. *Inorg. Chim. Acta* **1977**, *21*, 119.

(39) Bernarducci, E.; Bharadwaj, P. K.; Krogh-Jespersen, K; Potenza, J. A.; Schugar, H. J. *J. Am. Chem. Soc.* **1983**, *105*, 3860.

(40) The two low-lying states corresponding to alternative occupancies of the t_{2g} orbital set appear at 2400 and 2600 cm^{-1}, supporting the contention that the $4d_{xz}$ orbital is the singly occupied d-orbital in the ground state.

nature of the orbital in which the d-vacancy resides is best established experimentally by single-crystal EPR studies; such data are not currently available for **1**. However, EPR data are available for a mixed valence $(NH_3)_5Ru(pyrazine)Ru(NH_3)_5^{5+}$ ion ("Creutz-Taube ion"), which is crystallographically similar to **1** in that the pyrazine ring is staggered with respect to both $Ru(NH_3)_4$ units.[41] The unpaired electron mostly resides in an orbital perpendicular to the pyrazine plane, and delocalization over both Ru centers occurs via the $d(\pi)$ orbital on each Ru that participates in back-bonding with the pyrazine π^*-system. A recent combined EPR/MO study of Ru(III) complexes suggests that the half-occupied metal orbital tends to interact with a π-donor ligand.[42] This result implies that the Ru(III) d-vacancy in **1** (d_{xz}) is oriented so as to overlap favorably with the imidazole $p(\pi)$ system.

Concluding Remarks

The highly anisotropic lowest energy optical electron transfer absorption of **1** and the intimate electronic structural features of this chromophore have been characterized by the above spectroscopic and computational studies. These studies have quantified the intuitive expectation that the $d(\pi)/p(\pi)$ overlap between the Ru(III) d_{xz} orbital and the imidazole π-system must be strongly orientation dependent. In general, the same orbitals are involved in optical charge transfer (LMCT or MLCT) as in thermal electron transfer. Thus, an anisotropic optical electron transfer process implies that the rate of the corresponding thermal electron-transfer reaction should be sensitive to the orientation of the relevant donor/acceptor orbitals. The orientational dependence of long-range ("non-adiabatic") electron transfer on the electronic coupling between donor and acceptor orbitals is a topic of substantial current interest.[43-46] Our studies of **1** have the following implications for the use of $(NH_3)_5Ru^{III}$(his) as a probe of metalloprotein electron transfer: (1) The effective distance from a protein active site such as an Fe(II) heme to the probe should be that calculated to the *imidazole edge*. Owing to the strong electronic coupling between Ru(III) and the imidazole ligand, an electron transferred from the Fe(II) heme to the probe is "home free" once it reaches the imidazole edge. (2) The orientation of the $(NH_3)_5Ru^{III}$(his) unit relative to neighboring aromatic residues involved in electron-transfer pathways may strongly affect the rate of electron transfer.

Acknowledgment. The research of H.J.S. and J.A.P. was supported in part by the National Science Foundation (Grant CHE-8417548), the David and Johanna Busch Foundation, and the National Institutes of Health (the diffraction/crystallographic computing facility at Rutgers was purchased with Grant 1510 RRO 1486 O1A1). The research of K.K.-J. was supported by the National Institutes of Health (Grant GM-34111) and the donors of the Petroleum Research Fund, administered by the American Chemical Society. We thank Prof. S. Isied for a sample of the title complex and for helpful discussions. The computational studies benefited from electronic structure programs kindly supplied by Drs. M. Zerner and M. Krauss and from a grant of computer time from the Rutgers Center for Computer and Information Services.

Registry No. 1, 110528-80-8; $(NH_3)_5Ru$-imidazole^{3+}, 80593-52-8; $(NH_3)_5Ru$-4-methylimidazole^{3+}, 91209-01-7; $Ru(NH_3)_6^{3+}$, 18943-33-4; NH_3, 7664-41-7; imidazole, 288-32-4; 5-methylimidazole, 822-36-6.

Supplementary Material Available: Tables of hydrogen atom parameters and anisotropic thermal parameters (2 pages); listing of observed and calculated structure factors (7 pages). Ordering information is given on any current masthead page.

(41) Stebler, A.; Ammeter, J. H.; Furholz, U.; Ludi, A. *Inorg. Chem.* **1984**, *23*, 2764.
(42) Sakayi, S.; Yanase, Y.; Hagiwara, N.; Takeshita, T.; Naganuma, H.; Ohyoshi, A.; Ohkubo, K. *J. Phys. Chem.* **1982**, *86*, 1038.
(43) Siders, P.; Cave, R. J.; Marcus, R. A. *J. Chem. Phys.* **1984**, *81*, 5613.
(44) Ohta, K.; Closs, G. L.; Morokuma, K.; Green, N. J. *J. Am. Chem. Soc.* **1986**, *108*, 1319.
(45) Makinen, M. W.; Schichman, S. A.; Hill, S. C.; Gray, H. B. *Science* **1983**, *222*, 929.
(46) Closs, G. L.; Calcaterra, L. T.; Green, N. J.; Penfield, K. W.; Miller, J. R. *J. Phys. Chem.* **1986**, *90*, 3673.

Rhenium Carbonyl Semiquinone Complexes. Photochemical Addition of 9,10-Phenanthrenequinone to $Re_2(CO)_{10}$

Lynn A. deLearie and Cortlandt G. Pierpont*

Contribution from the Department of Chemistry and Biochemistry, University of Colorado, Boulder, Colorado 80309. *Received January 26, 1987*

Abstract: The photochemical reaction between $Re_2(CO)_{10}$ and 9,10-phenanthrenequinone has been investigated. In contrast with related reactions carried out with other quinones which gave tris(catecholate)rhenium(VI) products, the product obtained in this case is a binuclear rhenium(I) semiquinone carbonyl complex, $Re_2(CO)_7(PhenSQ)_2$. The complex crystallizes in the triclinic space group $P\bar{1}$ in a unit cell with dimensions a = 9.509 (2) Å, b = 11.955 (2) Å, c = 15.131 (4) Å, α = 74.36 (2)°, β = 87.20 (2)°, γ = 67.00 (2)°, and Z = 2. The binuclear complex consists of $Re(CO)_4(PhenSQ)$ and $Re(CO)_3(PhenSQ)$ units linked by a bridge formed by one semiquinone oxygen of the chelated ligand of the $Re(CO)_4(PhenSQ)$ unit. This oxygen bridges to the vacant coordination site of the $Re(CO)_3(PhenSQ)$ unit. Strong intramolecular interactions between semiquinone ligands further stabilize the dimeric structure in the solid state. This compound is paramagnetic in solution but diamagnetic in the solid state due to magnetic coupling between semiquinone ligands. Electrochemistry shows both chemically reversible two-electron reduction and oxidation couples. Mechanistic implications for the formation of this dimer and the previously characterized tris-chelated rhenium(VI)–catecholate complexes, $Re^{VI}(3,5\text{-}DBCat)_3$ and $Re^{VI}(Cl_4Cat)_3$, are discussed.

The photochemistry of binuclear metal carbonyl complexes has been studied in the course of investigating routes to reactive metal complexes. Several reports have appeared on reactions of dimanganese and dirhenium decacarbonyl which describe either homolytic cleavage of the metal–metal bond to give the $M(CO)_5$ radical[1] or heterolytic displacement of a carbonyl ligand to give

0002-7863/87/1509-7031$01.50/0